PREPARATION AND CHARACTERIZATION OF PHOTOCATALYTICALLY ACTIVE BISMUTH IODATE

[1,2]Vlastimil MATĚJKA, [2]Petr MARŠOLEK, [2]Alexandr MARTAUS, [3]Lucie GEMBALOVÁ, [1,2]Petr PRAUS

[1]VSB - Technical University of Ostrava, Faculty of metallurgy and materials engineering, Department of Chemistry, Ostrava, Czech Republic, EU, vlastimil.matejka@vsb.cz
[2]VSB - Technical University of Ostrava, Institute of Environmental Technology, Ostrava, Czech Republic, EU, petr.marsolek@vsb.cz
[3]VSB - Technical University of Ostrava, Faculty of Mining and Geology, Faculty of Mining and Geology, Institute of Clean Technologies for Mining and Utilization of Raw Materials for Energy Use, Ostrava, Czech Republic, EU, lucie.gembalova@vsb.cz

Abstract

Bismuth iodate was prepared using a hydrothermal synthesis of $Bi(NO_3)_3 \cdot 5H_2O$ and I_2O_5. The time effect of the hydrothermal synthesis (4, 24, 48 and 72 h) on the structure, specific surface area (SSA) and morphology of bismuth iodate particles, their optical properties and photodegradation activity were studied. A major phase presented in the prepared samples was $BiIO_4$ of which crystallite size increased with the duration of the synthesis as revealed with X-ray powder diffraction method. The values of specific surface area decreased with increasing time of the thermal treatment. The particles size and their morphology changed from very fine particles stacked into fluffy agglomerates observed after 4 h to agglomerates of tabular particles observed after 72 h long synthesis. The photocatalytic performance of the prepared samples irradiated with UVA light was evaluated by the photodegradation of model organic dye acid orange 7. It was observed that with the increasing duration of the $BiIO_4$ synthesis the photodegradation activity of resulting samples decreased. The photodegradation activity of $BiIO_4$ prepared at 4 and 24 h was higher than that of TiO_2 P25 (Degussa).

Keywords: Bismuth iodate, hydrothermal synthesis, characterization, photocatalysis

1. INTRODUCTION

The photocatalytic degradation of hazardous substances in water and air is part of perspective and widely studied methods mainly due to the fact that only an appropriate photocatalyst and light source of suitable wavelength is necessary. Titanium dioxide especially in its anatase form is undoubtedly the most studied material used for this purpose [1,2]. The band gap energy of anatase is approximately 3.20 eV what means this photocatalyst can be activated with light having wavelength equal to or lower than 387 nm what means it can be activated by UVA irradiation. Nowadays, many efforts are focused on the preparation of photocatalysts active in visible region of spectra, for example, intensively studied graphitic carbon nitride ($g\text{-}C_3N_4$) [3,4]. Efficient photocatalysts activated also by artificial UV light are still on high demand. The searching for new photocatalysts mainly reflects the demand for higher photodegradation efficiency, especially shifted towards the visible region [5].

It was already proved that the different bismuth based compounds, such as $BiVO_4$ [6], Bi_2WO_6 [7], Bi_2O_3 [8], exhibit high photodegradation efficiency, probably ascribed to lone pair electrons of Bi^{3+} [9]. $BiIO_4$ with layered structure is one of promising photocatalytically active semiconductors with the band gap energy close to that of TiO_2 [10,11]. Its layered structure is favorable for the efficient separation of electrons and holes and in general, this feature predetermines the layered photocatalytically active materials as the efficient photocatalysts.

In this research we focused on the synthesis of the $BiIO_4$ photocatalysts using the hydrothermal synthesis of aqueous solutions of $Bi(NO_3)_3 \cdot 5H_2O$ and I_2O_5. The prepared samples were characterized using X-ray powder diffraction method. Specific surface area was measured using the BET method; morphology of the particles was studied using scanning electron microscopy and band gap energy was determined using UV-VIS diffuse reflectance spectroscopy. The photodegradation activity of the prepared samples was evaluated by the UV induced photodegradation of azo dye acid orange 7.

2. MATERIALS AND METHODS

2.1. BiIO4 synthesis

$Bi(NO_3)_3 \cdot H_2O$ was obtained from Penta s.r.o., I_2O_5 was obtained from Sigma Aldrich, distilled water was used for all of the experiments. The weighted amounts of $Bi(NO_3)_3 \cdot 5H_2O$ and I_2O_5 were dissolved separately in distilled water with assistance of ultrasound. The resulting solutions were mixed together to reach a weight ratio of 1:3 of pure $Bi(NO_3)_3 \cdot 5H_2O$ and I_2O_5. The resulting mixture was further mixed using an electromagnetic stirrer for 1 h. After this step, the reaction mixture was treated in an autoclave at 150 °C for 4, 24, 48 and 72 h. The resulting white slurry was filtered and washed with distilled water and dried at 60 °C. Resulting coarse particles were pulverized using an agate mortar to give the final samples assigned as $BiIO_4(4)$, $BiIO_4(24)$, $BiIO_4(48)$ and $BiIO_4(72)$, respectively.

2.2. Characterization methods

The X-ray powder diffraction (XRPD) examination of the samples was performed on a SmartLab diffractometer (Rigaku, Japan) equipped with a detector D/teX Ultra 250. Cobalt tube (CoKα, λ_1 = 0.178892 nm, λ_2 = 0.179278 nm) operated at 40 kV and 40 mA was used as an irradiation source. The powder samples pressed in a silicon holder were measured in a reflection mode with the Bragg-Brentano geometry in a 2θ range of 5° − 90°, with a step size of 0.02° and speed of 1.5 deg·min^{-1}.

Specific surface area (SSA) of the samples was measured using an automated volumetric apparatus 3Flex (Micromeritics Instruments, USA) after sample degassing at 60 °C for 24 h at vacuum higher than 1 Pa. Nitrogen was used as an adsorbate and the adsorption-desorption isotherms of nitrogen were measured at −196 °C. The values of SSA were calculated according the Brunauer-Emmett-Teller (BET) theory for the range of relative pressure of 0.05-0.25.

UV-VIS diffuse reflectance spectroscopy (UV-VIS DRS) measurements were performed using a Shimadzu UV-2600 spectrometer (Shimadzu, Japan) equipped with an integrating sphere IRS-2600Plus (Shimadzu, Japan). The samples were pressed inside a holder and UV-VIS DRS spectra were acquired in the range of 300 - 500 nm. $BaSO_4$ powder (Nacalai Tesque, Inc., extra pure reagent grade) was used for a baseline setting. The Tauc's plots were used for the evaluation of indirect band gap energies [12].

Scanning electron microscopy (SEM) observations were conducted using a FEI Quanta 650 FEG microscope (FEI, USA). The powders were spread over a conductive tape attached to a sample holder and sputtered with chromium using Quorum Q150T ES (Quorum Technologies, Great Britain) to reach its layer thickness of approximately 35 nm. The particles were observed using a back scattered electron detector (BSE).

The photodegradation activity of prepared samples was tested by the UV induced photodegradation of acid orange 7 (AO7) (Synthesia, a.s.). In the typical experiment, the tested samples were weighted (0.0500 g) into a glass bowl filled with 150 ml of distilled water and mixed using an electromagnetic stirrer (300 rpm). After 5 min of stirring 15 ml of the AO7 solution (c = 7.136 10^{-4} mol dm^{-3}) was added. The resulting suspension was further stirred in dark for 1 h to achieve the adsorption equilibrium. After this period, 5 ml of suspension was taken and filtered through a syringe filter Chromafil PP/GF/RC-20/25 (Macherey-Nagel, Germany). The absorbance of filtered solutions was measured at 480 nm using a Shimadzu UV-2600 spectrometer and assigned as A_0. In the same time a source of UV light (BLB 36 W, NARVA) was turned on and the sample was

subjected to irradiation for 150 min. 5 ml of sample was taken out of the stirred suspension in selected time intervals (30, 60, 90 and 150 min) and filtered using a syringe filter. The absorbance of the filtered solution was measured at 480 nm; the values were assigned as A_{30}, A_{60}, A_{90} and A_{150}, respectively.

3. RESULTS AND DISCUSSION

X-ray powder diffraction analysis

The XRPD patterns of the synthesized samples $BiIO_4$(4), $BiIO_4$(24), $BiIO_4$(48) and $BiIO_4$(72) are compared in **Figure 1**. The phase $BiIO_4$ (01-080-7870) was identified as a major phase in all of the prepared samples. It is evident the intensity of the diffraction lines (0 1 0) and (0 4 2) are growing with duration of the hydrothermal synthesis.

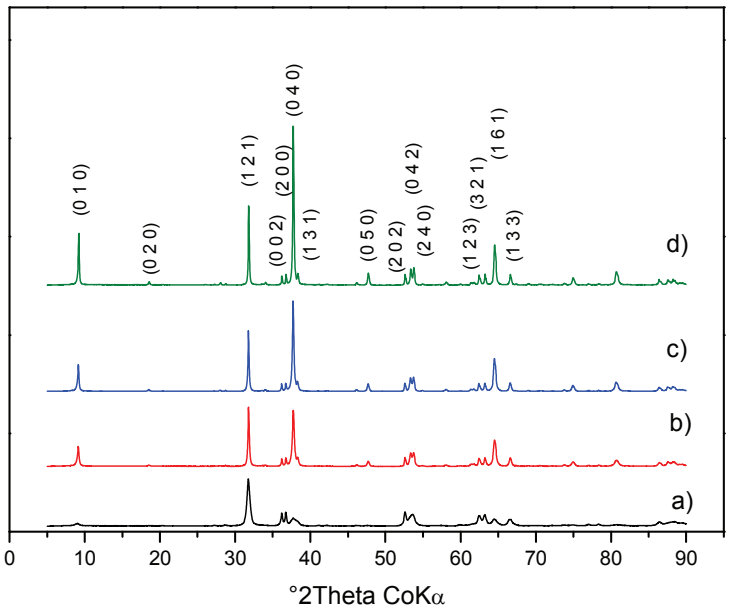

Figure 1 XRPD patterns of $BiIO_4$(4) (a), $BiIO_4$(24) (b), $BiIO_4$(48) (c) and $BiIO_4$(72) (d) samples

The sizes of the crystallites were calculated according to the Halder-Wagner equation implemented in the evaluation software PDXL2 (Rigaku, Japan) and are listed in **Table 1**.

Table 1 The values of crystalite size (L_D), specific surface area (SSA), band gap energy (Eg)

Sample	L_D (nm)	SSA ($m^2 \times g^{-1}$)	Eg (eV)
BiIO4(4)	20	16	3.20
$BiIO_4$(24)	30	11	3.20
$BiIO_4$(48)	39	6	3.17
BIO_4(72)	52	7	3.17
TiO_2 P25	Anatase - 20; Rutile - 29	50	3.20

The intensities of the diffraction lines obtained for the samples $BiIO_4$(4) and $BiIO_4$(24) are closely similar with that reported for $BiIO_4$ (JCPDS 01-080-7870). For the samples $BiIO_4$(48) and $BiIO_4$(72) the significantly higher intensity was registered for the diffraction peak (0 4 0) in comparison to that reported in its PDF card (JCPDS 01-080-7870) which could be attributed to preferential growing of the $BiIO_4$ crystals in this direction. The XRPD diffraction pattern of TiO_2 P25 (not shown in **Figure 1**) revealed the presence of anatase (A) and rutile (R) with

the crystallite sizes of 20 and 29 nm, respectively. The calculated weight proportion of anatase and rutile in the P25 sample was 80 : 20.

The dependency of optical reflectance of the sample powders on wavelength was measured using UV-VIS DRS and is shown in **Figure 2**. The appropriate Tauc´s plots for indirect transitions are shown in **Figure 3** and the determined band gap energies are listed in **Table 1**.

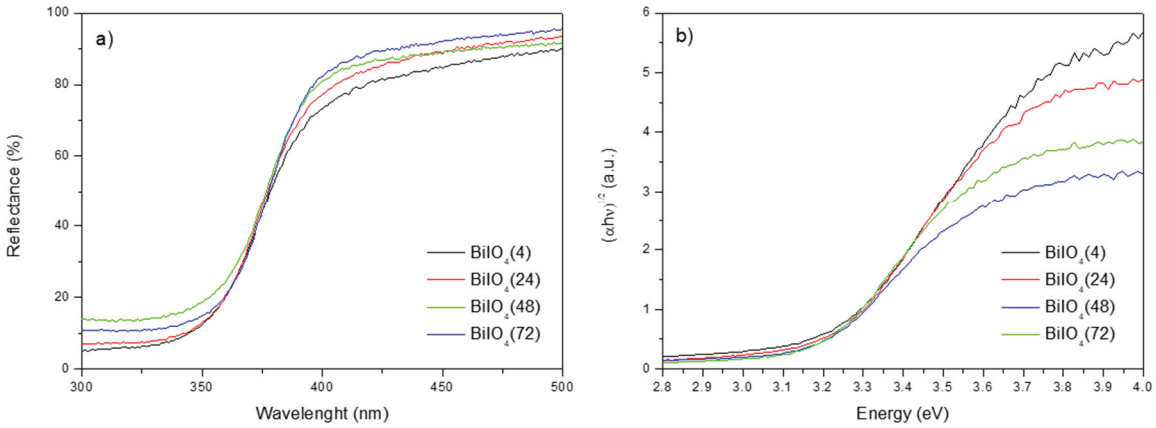

Figure 2 UV-VIS DRS spectra (a) and Tauc´s plots (b) of $BiIO_4$(4), $BiIO_4$(24), $BiIO_4$(48) and $BiIO_4$(72)

The obtained values of E_g for the samples $BiIO_4$(4) and $BiIO_4$(24) are the same as that obtained for P25 and indicate the photocatalytic activity could be activated with irradiation having the wavelength ≤ 387 nm. The E_g values obtained for the samples $BiIO_4$(48) and $BiIO_4$(72) reached slightly lower values and the photocatalytic properties of both materials could be activated with UV irradiation having the wavelength ≤ 391 nm. The E_g values obtained for the synthesized samples were higher than that (2.94 eV) published by Huang et al [11].

The SEM images of the samples BiIO4(4) and BiIO4(72) obtained using SEM operated in a back scattered electron mode are shown in **Figure 3**. The $BiIO_4$(4) sample (**Figure 3a**) occurred as fluffy aggregates of very fine particles contrary to the aggregates of particles of the BiIO4(72) sample which appeared as needles and also small plates which is evident from **Figure 3b**. The bigger particle size was evidenced for the sample $BiIO_4$(72) (see **Figure 3b**). Growing intensity of the diffraction peaks (0 X 0) with the duration of the hydrothermal synthesis was identified by the XRPD method (**Figure 1**) and correlates with the observations achieved by the SEM method where the needle like shaped particles were observed.

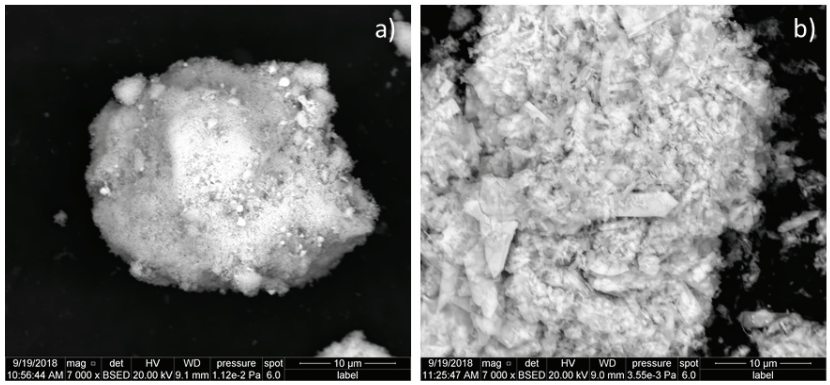

Figure 3 SEM images of $BiIO_4$(4) (a) and $BiIO_4$(72) (b) samples

The UV induced photodegradation activity of the prepared samples against AO7 is graphically presented in **Figure 4** and in the same figure it is compared with the photodegradation activity of TiO_2.

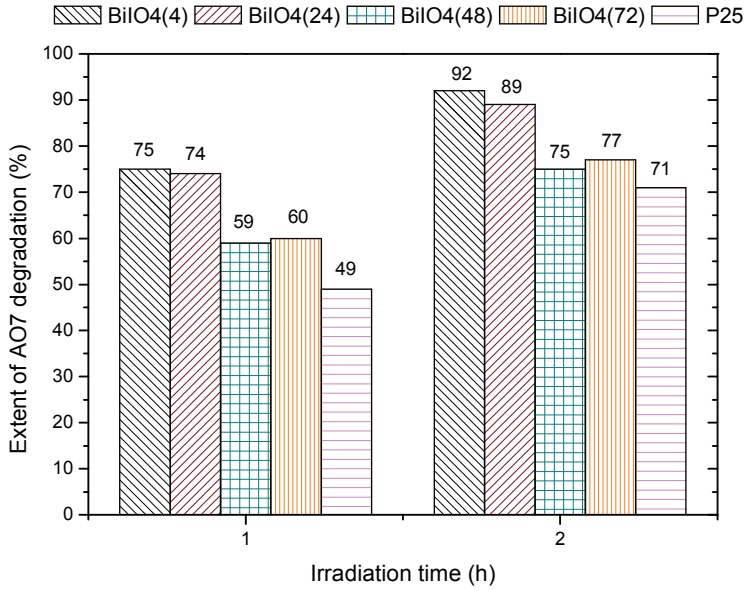

Figure 4 Photodegradation bars of AO7 for $BiIO_4(4)$, $BiIO_4(24)$, $BiIO_4(48)$, $BiIO_4(72)$ and TiO_2

Figure 4 indicates that more than 70 % of AO7 was degraded with the samples $BiIO_4(4)$ and $BiIO_4(24)$ after 1 h of irradiation. Approximately 60 % of AO7 was degraded with $BiIO_4(48)$ and $BiIO_4(72)$ and only 50 % of AO7 was degraded with TiO_2 after 1 h of irradiation. After 2 h of irradiation approximately 90 % of AO7 was photodegraded in case of the samples $BiIO_4(4)$ and $BiIO_4(24)$. Less than 80 % of AO7 was removed with the samples $BiIO_4(48)$, $BiIO_4(72)$ and TiO_2. Looking at the **Table 1** there is the correlation between crystallite size, SSA and the photodegradation activity of $BiIO_4$ samples: the lower the value of L_D, was the higher the value of SSA was and the photodegradation activity increased. The results pictured in **Figure 4** indicate the $BiIO_4(4)$ and $BiIO_4(24)$ samples as perspective photocatalysts for the photocatalytic degradation of azo dyes.

4. CONCLUSION

The samples of $BiIO_4$ were successfully prepared using the hydrothermal synthesis of the aqueous solutions of $Bi(NO_3)_3 \cdot 5H_2O$ and I_2O_5. It was observed that the different synthesis time had the effect on the structure, texture, morphology and photodegradation activity of the resulting samples. The results of photodegradation experiments indicated the samples synthesized for 4 and 24h were of the best photocatalytic degradation efficiency of AO7 reaching approximately 90 % after 2 h of UV irradiation. It is obviously higher than the performance of TiO_2 of which the extent of AO7 degradation reached 71 %.

Bismuth iodates are promising nanomaterials for photocatalytic applications and further research will be focused on shifting their photodegradation activity towards visible region by preparing nanocomposites with g-C_3N_4. The photocatalytic activity of both $BiIO_4$ and its nanocomposites with g-C_3N_4 will be also tested for degradation of various substances.

ACKNOWLEDGEMENTS

This work was supported by the Grant Agency of the Czech Republic (reg. No. 16-10527S) and by the student projects SP2018/79 of VSB-Technical University of Ostrava.

REFERENCES

[1] LEE, S.-Y. and PARK S.-J. TiO2 photocatalyst for water treatment applications. *Journal of Industrial and Engineering Chemistry*. 2013, vol. 19, no. 6, pp. 1761-1769.

[2] REN, H., KOSHY, P., CHEN, W.-F., QI, S. and SORRELL, C.C. Photocatalytic materials and technologies for air purification, *Journal of Hazardous Materials.* 2017, vol 325, pp. 340-366.

[3] XU, B., BOSHIR AHMED, M., ZHOU, J.L., ALTAEE, A., XU, G. and WU, M. Graphitic carbon nitride based nanocomposites for the photocatalysis of organic contaminants under visible irradiation: Progress, limitations and future directions. *Science of The Total Environment*. 2018, vol. 633, pp. 546-559.

[4] MASIH D., MA Y. and ROHANI, S. Graphitic C3N4 based noble-metal-free photocatalyst systems: A review. *Applied Catalysis B: Environmental.* 2017, vol. 206, pp. 556-588.

[5] SHAHAM-WALDMANN, N. and PAZ, Y. Away from TiO2: A critical minireview on the developing of new photocatalysts for degradation of contaminants in water. *Materials Science in Semiconductor Processing.* 2016, vol.48 Part 1, pp. 72-80.

[6] VENKATESAN, R., VELUMANI, S., ORDON, K., MALOWSKA-JANUSIK, M., CORBEL, G. and KASSIBA, A. Nanostructured bismuth vanadate (BiVO4) thin films for efficient visible light photocatalysis, *Materials Chemistry and Physics.* 2018, vol. 205, pp. 325-333.

[7] SELVI, M.H., VANGA, P.R. and ASHOK M. Photocatalytic application of Bi2WO6 nanoplates structure for effective degradation of methylene blue. *Optik.* 2018, vol. 173, pp. 227-234.

[8] RAZA, W., HAQUE M.M., MUNEER, M., HARADA, T. and MATSUMA, M. Synthesis, characterization and photocatalytic performance of visible light induced bismuth oxide nanoparticle. *Journal of Alloys and Compounds.* 2015, vol. 648, pp. 641-650.

[9] LI, F., HOU, X., PAN, S. and WANG, X. Growth, Structure, and Optical Properties of a Congruent Melting Oxyborate, Bi2ZnOB2O6. *Chemistry of Materials.* 2009, vol. 21, no. 13, pp. 2846-2850.

[10] HUANG, H., LIU, L., ZHANG, Y. and TIAN, N. One pot hydrothermal synthesis of a novel BiIO4/Bi2MoO6 heterojunction photocatalyst with enhanced visible-light-driven photocatalytic activity for rhodamine B degradation and photocurrent generation. *Journal of Alloys and Compounds.* 2015, vol. 619, pp. 807-811.

[11] HUANG, H., HE, Y., HE, R., JIANG X., LIN, Z., ZHANG, Y. and WANG S. Novel Bi-based iodate photocatalysts with high photocatalytic activity. *Inorganic Chemistry Communications.* 2014, vol. 40, pp. 215-219.

[12] TAUC, J., GRIGOROVICI, R. and VANCU, A. Optical Properties and Electronic Structure of Amorphous Germanium. *Physica Status Solidi (b).* 1966, vol. 15, no. 2, pp. 627-637.